Evaluating and Modeling the Effect of Frame Rate on Steering Performance in Virtual Reality

Yushi Wei, Rongkai Shi, Anil Ufuk Batmaz, *Member, IEEE*, Yue Li, Mengjie Huang, Rui Yang and Hai-Ning Liang, *Member, IEEE*

Abstract— Prior work has shown that frame rate significantly influences user behavior in fast-response tasks in 2D and 3D contexts. However, its impact on a steering task, which involves navigating an object along a path from the start to the end, remains relatively unexplored, especially in the context of virtual reality (VR). This task is considered a typical non-fast-response activity, as it does not demand rapid reactions within a limited time frame. Our work aims to understand and model users' steering behavior and predict movement time with different task complexities and frame rates in VR environments. We first conducted a user study to collect user behavior in a steering task with four factors: frame rate, path length, width, and radius of curvature. Based on the results, we then quantified the effects of frame rate and built two predictive models. Our models exhibited the best fit ($r^2 > 0.957$) and over 17% improvement in prediction accuracy for movement time compared to existing models. Our models' robustness was further validated by applying them to predict steering performance with different VR tasks and frame rates. The two models keep the best predictability for both movement time and speed.

Index Terms—Virtual reality; human performance modeling; steering law; frame rate; head-mounted display

1 Introduction

Path steering is one of the most common and fundamental tasks in both 2D and 3D scenarios. In this task, the user is required to move an object, like a cursor, stylus, or controller-based pointer, along the entire length of a path with different shapes. Specifically, steering tasks are manifested in numerous contexts, such as implementing sliding and navigation features in touch screen applications [30], integrating gesture recognition techniques in mobile applications [49], and using brush control mechanisms in graphic design software [33].

To gain a deeper understanding of user behavior in steering tasks, Accot and Zhai [3] introduced the steering law model, which is derived from Fitts' law and is intended to help predict movement time (MT). Their model effectively explains the effects of path length and width on MT. However, due to the increasing diversity of interaction tasks, the explanatory capacity of the original steering law model has become inadequate to meet the demands of more contemporary tasks. Therefore, various refined models built upon the original steering law paradigm have been proposed to cover more specific attributes such as path scale and curvature [62, 66]. These refined models extend the applicability of the steering law to a broader array of contexts, enhancing its predictive and explanatory power for MT.

Since steering law tasks are very common on 2D touchscreens or monitors (e.g., smartphones and personal computers), most proposed models primarily focus on interactions within the 2D context. Recently, virtual reality (VR) head-mounted display (HMD) technologies have witnessed rapid growth. VR HMDs immerse users in interactive digital 3D environments that simulate real-world experiences. The immersive 3D virtual environments (VEs) provide unique interactions and experiences that are significantly different from conventional 2D surface interactions [27, 70]. This technological progress has expanded to various fields, including gaming [32], training [61], education [28], and medicine [34, 51]. However, the suitability of steering law in such 3D task environments and its validity in VR HMDs have still not been thoroughly investigated.

Compared to 2D interaction scenarios, in addition to their inherent interactivity, there are other factors that may significantly affect user interaction behavior and experience in VR HMDs. One of these factors is the frame rate [55], i.e., the number of discrete images shown to the user's eyes per second, measured in frames per second (fps). A monitor's maximum achievable frame rate is constrained by its refresh rate (measured in Hertz, Hz), which refers to the number of times per second the monitor can refresh the screen [38]. The variability in frame rates can result in different levels of latency [56]. While latency and frame rates are not directly equivalent, previous research has demonstrated that lower frame rates tend to be associated with higher visual lag [56]. Specifically, frame rate and the latency it caused in a VR system would affect user motor performance [45]. A low frame rate and the accompanying latency might weaken users' ability to execute precise movements, experience immersion, and interact effectively with VE. First, low frame rates hinder the accuracy of fine motor control, undermining users' ability to judge and adjust their movements accurately [56]. Second, Claypool et al. [17] showed that users' responsiveness decreased due to low frame rates, causing a disconnect between real-world actions and virtual feedback. Further, the learning processes can also be hampered, limiting the acquisition of motor skills and muscle memory [72]. In scenarios where real-time decision-making and precise motor control are crucial, such as virtual surgery simulations, safety can be compromised by low frame rates [48, 72].

Besides, frame rates brought more challenges to immersive 3D VEs in VR HMDs. Within an immersive VE, the frame rate exerts a more pronounced influence on user behavior compared to using a 2D screen-based device [55], of which the screen's frame rate only influences a limited interaction space while the frame rate controls and influences all the rendered visual elements surrounding the users in an immersive VE. On the other hand, the impact of the frame rate is non-uniform and uncertain due to the diversification of VR headsets. The default refresh rate of a headset equipped with differs, as summarized in Fig. 1. Moreover, frame rates in practical applications are often reduced and fluctuating because of the hardware device performance limitations and

- *Yushi Wei, Rongkai Shi, and Hai-Ning Liang are with the Computational Media and Arts Thrust in the Information Hub at The Hong Kong University of Science and Technology (Guangzhou), China.*
- *Anil Ufuk Batmaz is with the Department of Computer Science & Software Engineering at Concordia University, Canada.*
- *Yue Li is with the Department of Computing in the School of Advanced Technology at Xi'an Jiaotong-Liverpool University, China.*
- *Mengjie Huang is with the Department of Industrial Design in the Design School at Xi'an Jiaotong-Liverpool University, China.*
- *Rui Yang is with the Department of Intelligent Science in the School of Advanced Technology at Xi'an Jiaotong-Liverpool University, China.*
- *Hai-Ning Liang is the corresponding author. E-mail: hainingliang@hkust-gz.edu.cn.*

Manuscript received xx xxx. 201x; accepted xx xxx. 201x. Date of Publication xx xxx. 201x; date of current version xx xxx. 201x. For information on obtaining reprints of this article, please send e-mail to: reprints@ieee.org. Digital Object Identifier: xx.xxxx/TVCG.201x.xxxxxxx

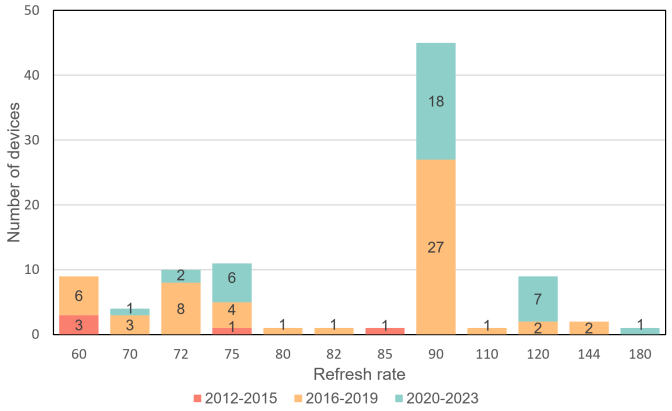

Fig. 1: A stacked bar chart depicting the quantity of VR HMDs by refresh rates, categorized by their released dates [12].

programs' complexity. This reduction and fluctuation can occur, for instance, in scenarios where the game scene is highly complex or when running programs with extensive computational demands.

In summary, while some studies have investigated the influence of frame rate and the caused visual lag on human behavior in immersive 3D VEs, these studies have primarily focused on tasks that require rapid responses within short time frames. In such contexts, achieving superior performance needs immediate reaction and action, as illustrated in games like Fruit Ninja and First Person Shooter, where participants must swiftly cut fruits or shoot enemies as soon as they appear on the screen [44, 55]. The time constraints inherent in these tasks inevitably impose mental pressure on users, limiting their capacity to perceive and interact with objects in the surrounding environment, which has been demonstrated can significantly affect human behaviors and the final results in human factor-based research [63, 68]. Thus, these findings are not directly transferable to non-fast-response tasks where users have the flexibility to decide the interaction process without any time-limited requirements, such as menu manipulation and object relocation. [1] Therefore, when validating the applicability of the steering law, a typical non-fast-response task, in VR HMDs, it is necessary to reconsider the effect of frame rate. This would improve the accuracy and usefulness of systems created by practitioners, designers, and engineers.

In this paper, to confirm the applicability of the steering law in immersive VR environments and refine the original model to have stronger prediction capabilities at varying frame rates, a user study ($N = 24$) was conducted to examine how factors including path length, width, curvature radius, and frame rate could affect movement time, success rate, and average movement speed during the steering task (Sec. 4). According to the collected data, we quantified the effects of frame rate and proposed two refined predictive models (Sec. 5). Finally, we conducted another user study ($N = 15$) to collect more user behavior data within a tracing task to compare our models with those showing the best performance in previous works (Sec. 6). The results demonstrated that our models have the highest predictive accuracy for both movement time and average movement speed.

In short, our contributions are:

- Empirically demonstrate the influence of frame rate on user behavior within the context of steering tasks.
- Ascertain that user behavior in VR steering tasks, much like in 2D scenarios, is significantly affected by path length, width, and curvature.
- Confirm the suitability of the steering law model in immersive VR environments.
- Introduce two novel models that predict users' movement time and speed under varying frame rates and path characteristics.

[1] In this paper, non-fast response tasks refer to tasks that do not have a high cognitive demand for users to react and respond in a short interval of time. Please note that the completion time of fast-response tasks is typically short, while the completion time of non-fast-response tasks does not have to be long. That said, the total time required for task completion is not a criterion for distinguishing between these two types of tasks.

2 Related Work

In this section, we delve into diverse models derived from the steering law, adapted to address distinct application-specific scenarios. We subsequently provide a concise overview of the resultant impact stemming from frame rate fluctuations on users' behavior, which inspired us to build our frame-rate-based models.

2.1 Steering Law

Movement time MT, representing the duration from the initiation of movement for the selection to the completion, is one of the most commonly used metrics for evaluating users' performance in different tasks. MT was first modeled by Fitts' law [23]—the well-known model used to predict users' motor behaviors and time spent during the pointing selection process based on the index of difficulty (ID), which is calculated using target width (W) and amplitude (A) (see Eq. (1) [36]).

$$MT = a + b \cdot ID = a + b \log_2 \left(\frac{A}{W} \right) \tag{1}$$

While Fitts' law delineates the relation between MT and ID for pointing tasks exclusively, Accot and Zhai [3] further proposed the steering law that retains the purpose of Fitts' law but generalizes it to trajectory-based movement unconstrained by path configurations, such as a path with a spiral, circular, or constrained shape (see Eq. (2)).

$$MT_C = a + b \cdot ID = a + b \int_C \frac{dx}{W(x)} \tag{2}$$

In Eq. (2), a and b are empirical constants, C is defined as the path length parameterized by x, and $W(x)$ signifies the path width at specified position x. Eq. (2) is denoted as the 'global law' predicting the aggregate temporal duration requisite for the steering procedure. In case the path is straight and has a constant width, the model can be simplified as:

$$MT = a + b \frac{A}{W} \tag{3}$$

Based on this first modeling for straight paths, researchers have proposed several extended models to explain the steering behavior for irregular paths. For example, Liu et al. [35] conducted two user studies to evaluate, validate, and model how the curvature radius R and orientation can impact the steering performance in desktop-based 3D VEs. Their results showed that an increased path curvature would proportionately prolong the task completion time, which is consistent with previous work on Fitts' law [9]. Moreover, in terms of the influence exerted by curvature on the celerity of locomotion, Montazer et al. [39] demonstrated a positive correlation between speed V and curvature radius R. The correlation has also been substantiated empirically by Nancel and Lank [42], who further proposed a refined model considering the effect of arbitrary curvature variations along constrained paths. They employed kinematic theory, two-thirds power law, and minimum jerk model in the steering law [24, 31, 53]. Although the same trend has been proven by the aforementioned works [35, 39, 42], there is still a lack of consistent formulations regarding the curvature radius R. Therefore, Yamanaka and Miyashita [66] posited their model (see Eq. (4), c and d in the equation are another two empirical constants) to better understand human steering processes and behavioral patterns with different R through a more consistent approach, demonstrating a superior capability of predicting MT for various steering behaviors.

$$MT = a + b \frac{A}{W + c(1/R) + dW(1/R)} \tag{4}$$

2.2 Application of Steering Law in 2D and 3D Environments

The role of trajectory-based steering tasks, such as pursuit tracking, drawing, and writing, has become increasingly important in the last decade. There have been extensive discussions about applying the steering law in 2D user interfaces (UIs) and applications, such as optimizing hierarchical menus [6], introducing force feedback [20], and understanding the effects of scale [5], start position [71], and devices in steering tasks [4,46]. Though some work has studied steering law in 3D UIs, there is limited understanding of applying it in immersive VEs. For example, Zhai et al. [69] have applied the formula in a locomotion task within a VE simulated through a conjunct of contiguous 2D projections fully enveloping participants. Nonetheless, this approach cannot be considered an optimal immersive VR configuration, given the interaction discrepancies between HMDs-based and 2D-based VEs [15,40,59].

Even though the steering law has been deeply investigated and applied in 2D applications, the virtual environment, such as interacting with objects at different depth planes, and the limitations of the VR HMDs, such as nonphysical support of mid-air interaction and stereo deficiencies, raises new challenges for steering law in 3D. Thus, researchers, such as Liu et al. [35], extended the steering law to 3D environments. However, due to technological limitations, the scope of their study was constrained exclusively to desktop-based 3D VEs [35]. The disparities between two types of VEs have already been demonstrated [10]. Furthermore, several studies have used the steering law in VEs primarily as an analytical tool to assess user performance without explicitly addressing its inherent applicability within VEs. For instance, Monteiro et al. [41] used the steering law to evaluate and compare the performance of various VR navigation interfaces. Similarly, Wolf et al. [60] examined input methods for circular steering tasks in augmented reality (AR) HMDs.

Therefore, considering the absence of previous research in rigorously evaluating the steering law in fully immersive VEs and the limited understanding of its suitability within 3D UIs, there is a compelling need for further investigation. It is crucial to delve into the implications of applying the steering law within VEs and devise strategies to effectively adapt it to accommodate the distinctive attributes of VR HMD devices and 3D UIs.

2.3 Frame Rate, Refresh Rate, and Latency

Frame rate and refresh rate are commonly used to represent the extent of smoothness and continuity of display and interaction [73]. The upper threshold of the display refresh rate and the maximum rendering frame rate frequency of the graphics card (GPU) typically constrain the maximum level of perceptible displaying smoothness by the naked eye [25,55]. Moreover, the impact of latency on user behavior and performance is typically associated with frame rate, where higher frame rates generally lead to lower visual lag [55,56]. Unlike the unstable latency caused by the program or hardware performance, this visual delay raised by frame rate is usually fixed and only affected by the rendering frequency between two frames [13].

Nowadays, considerable attention has been devoted to determining the minimum frame rate requirements for optimal human performance across various tasks. The frame rate with high rendering frequencies typically requires high-performance hardware, such as a high-capacity GPU and a high refresh rate display, which can often entail substantial costs [14,55]. Currently, several studies have identified 10 fps as the minimum threshold for human performance in 2D UIs and immersive VEs [13,37,57,58]. Although a 10-fps frame rate may suffice as a benchmark for certain applications, it should not be construed as applicable to all systems and applications. This is because the minimum frame rate requirements for optimal performance can vary substantially, such as grasping virtual objects with 7 Hz [43] and rendering complex graphics with 6 Hz [7], in accordance with the distinct content attributes.

More relevant to our research is that, with the upgrade of display technology and the increasing requirement for smoother and clearer displays [19,21], numerous researchers have paid attention to measuring the effects on users' behaviors between different performances of displays [17,50,54]. Typically, higher frame rates with lower fixed latency tend to result in reduced simulator sickness [29,55] and improved user performance in target-reaching tasks [56] and driving training [67]. For example, in PC first-person shooter video games, Claypool et al. [16] proved that frame rates below 30 fps can significantly decrease the player's experience and performance. Moreover, Claypool and Claypool [17] showed that user performance can vary up to seven times between 60 fps and frame rates ranging from 3 to 7 fps. This pattern is also demonstrated within 3D application scenarios. Wang et al.'s results indicated that users exhibited enhanced performance across various tasks when exposed to higher frame rates (e.g., 120 to 180 fps) in comparison to lower frame rates (e.g., 60 fps) [55]. It is worth noting that some studies showed results contrary to the aforementioned conclusions. For instance, Ware and Balakrishnan [56] indicated frame rates exceeding 10 fps did not significantly improve user performance for target localization tasks. Given that the aforementioned outcomes stem from diverse tasks and application contexts, they align with the earlier depiction that frame rates wield distinct effects on users' behaviors across various tasks and application scenarios. Consequently, engaging in a dedicated discourse and modeling the steering task within 3D immersive VEs is important, given the growing popularity of VR HMDs.

3 Research Questions

Although previous studies analyzed the effects of frame rate, they mostly focused on fast response or timing-limited tasks in 2D scenarios. In addition, they typically investigate to discover the minimal frame rate threshold for comfortable interactions or observe the behaviors only. However, the effects of frame rate on non-fast-response tasks have not been well discussed in both 2D and 3D contexts. To better understand whether frame rate has an impact on user behavior in non-fast-response tasks in immersive VEs, we collected user performance data in a steering task, a typical non-fast-response task, under different frame rates and path features. Our work aims to seek answers to the following research questions (*RQs*):

RQ1: Does the variation in frame rates exert an influence on users' performance in steering tasks in immersive VEs? Previous studies have presented divergent conclusions regarding the influence of frame rates on user behavior. The prevailing consensus among most investigations shows a positive correlation between user performance and frame rates [16, 18]. However, results from studies, e.g., Ware and Balakrishnan. [56], have indicated that no discernible association exists between frame rates and user performance when frame rates exceed a certain threshold. As described in Sec. 2.3, researchers considered this incongruity could be attributed to the disparate effects that varying frame rates exert on distinct tasks. In immersive VEs, although empirical evidence has established that higher frame rates enhance user performance, these findings are predominantly situated within gaming contexts [55]. Given the inherent distinctions between the steering task and typical gaming contexts, it is important to examine the applicability of such conclusions to the steering task paradigm.

RQ2: How do the path features, including path lengths, widths, and radii of curvature, affect user performance in a steering task in VR HMDs? Previous steering law research conducted in 2D environments has demonstrated that a reduced task difficulty caused by a smaller path curvature radius, a shorter or a wider path, generally resulted in improved user performance within speed and accuracy [5,42]. However, the applicability of these conclusions to immersive VR scenarios, which have different visualizations and input paradigms compared to 2D environments, remains unclear.

RQ3: How applicable is the steering law to immersive VEs? The steering law has been applied across various contexts in prior research, mostly in 2D environments [3, 5]. Although certain studies have incorporated its usage within 3D/VR environments, these instances have been hindered by technological limitations. Consequently, disparities persist between its application in those contexts and the contemporary immersive VEs [35, 69]. Moreover, while certain studies have taken into account the integration of the steering law paradigm within immersive VEs, this research has exclusively employed the steering law as an analytical tool without conducting individualized experimentation

and analyzing the steering law (e.g., [41,60]). Therefore, the unverified suitability of the steering law within immersive VEs requires further investigation.

RQ4: If the effect of frame rate is observed on users' behavior in steering tasks, can this effect be formalized through mathematical modeling? Refining models' performance by employing modeling to summarize the effect on users' performance is one of the most fundamental topics of human-computer interaction studies. Previous research has derived models and extended the steering law to various complex scenarios [62,66]. If the answers to *RQ1-3* confirm the existence of an impact from frame rates on user behavior, we also want to explore the feasibility of encapsulating user behavior through mathematical modeling. Such models will enhance the explanatory capacity of the steering law, thereby fostering a more robust comprehension of user behavior.

4 User Study

This user study aims to collect data on different categories for hand-based steering tasks at varied frame rates in VR HMDs. This allows us to understand better how the frame rates and path features (path length, width, and curvature radius) affect users' steering behaviors.

4.1 Participants

Twenty-four participants (14 females and 10 males) were recruited from a local university. Their ages ranged from 19 to 25 ($M = 20.325$, $SD = 1.378$). All participants could clearly see all objects in the scene. Ten of them had prior experience with VR HMDs for 0-5 hours per week, eight used the device for 5-10 hours per week, and six reported had never used a VR device before.

4.2 Apparatus

We used a Pimax 5K Super[2] for this study, which features a refresh rate of 180 Hz—exceeding that of all other currently available VR devices [55]. The headset has a resolution of 2560 × 1440 (2.5K) per eye, a horizontal field of view (FoV) of 170°, and a vertical FoV of 115°. We used a Windows 10 PC with an Intel Core i9 processor, 64 GB RAM, and an NVIDIA RTX 3090 graphic card, to power the VR HMD. The experimental program was implemented in C# in Unity3D (version 2022.3.01f) with SteamVR PlugIn (version 2.2.0). The participants used an HTC Vive controller for interaction, which was tracked by two SteamVR 2.0 Base Stations.

4.2.1 Eliminating the Potential Latency Effects

Three approaches were adopted to eliminate the potential effect caused by the additional latency, i.e., waiting for software or network processing and limited performance of hardware: (1) The Pimax 5K Super is equipped with a refresh rate of 180 Hz, which is higher than or equal to the frame rate conditions we set up (which we will introduce in Sec. 4.4). Thus, throughout the user study, the headset was capable of consistently and accurately rendering the VE in each frame rate condition without additional visual lag caused by the HMD. (2) Two SteamVR 2.0 Base Stations were employed to track hand motion during the task. Their tracking frequency reaches 1000 Hz, significantly surpassing the refresh rate of the headset [2]. This ensures rendering consistency and eliminates latency discrepancies between the controller and the HMD, even in high-frame-rate conditions in the user study. (3) The program is structured as a single-threaded procedure without network requirement by the Unity game engine, with all operations contained within the `Update()` function, which is invoked once per frame [1]. Briefly, in Unity, the `Update()` function precedes rendering, ensuring that all operations are processed before frames are rendered. More importantly, the experimental program was executed on a high-performance PC with robust hardware capabilities, which ensured that all data were processed in a time shorter than the interval between each frame [50]. This approach effectively minimizes the likelihood of varying delays at different frame rates.

[2] https://support.pimax.com/en/support/home

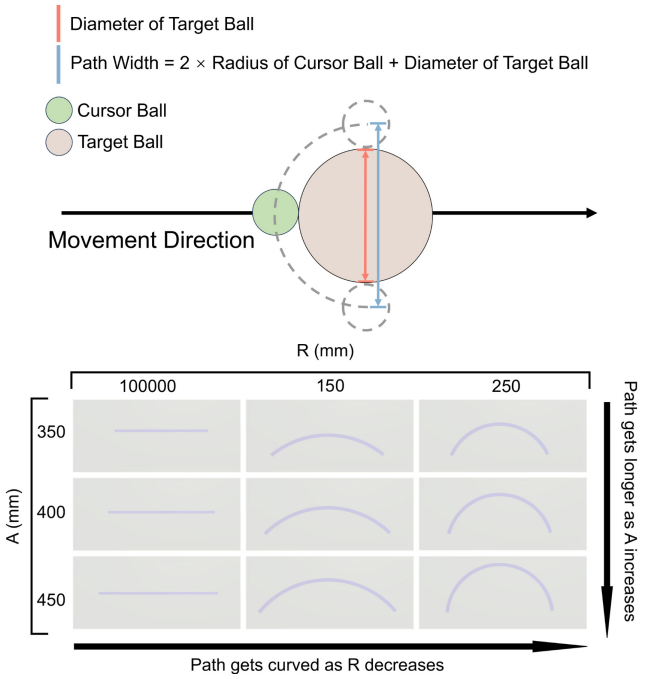

Fig. 2: The path width is defined by the sum of the diameters of the target ball and the cursor ball. The dotted lines represent where the cursor ball can be moved to push the target ball (TOP). The path configurations regarding curvature radii (R) and path lengths (A) (BOTTOM).

4.3 Task and Stimuli

In our work, we used a similar task described by Liu et al. [35]. Participants sat completing the given task. The task contained a steering mechanism employed in a VE. In each trial, a steering path was instantiated at a distance of 40 cm in front of the center of the participants' FoV. The target ball was attached to the steering law and positioned at its left end. The cursor ball was positioned directly in front of the controller with a diameter of 10 mm. In each trial, participants were required to control the cursor ball to push the target ball through the entire path (i.e., from the left initial to the right end). They received visual and haptic feedback based on the position of the target ball on the line and the occasion when the cursor and the target ball collided (the controller vibrates 0.1 s with each collision), respectively. The stimuli were ascertained by a pilot study for optimal suitability. During the trial, participants were not allowed to reset the process and repeat it anew within a single trial once it had commenced, regardless of their actual or perceived performance falling short of their expectations [62]. Additionally, participants were consistently instructed to prioritize both speed and accuracy while performing each trial.

4.4 Design and Procedure

The user study employed a $3 \times 2 \times 3 \times 8$ within-subjects design with four independent variables, resulting in 144 conditions in total:

- Path Length (A): 350 mm, 400 mm, and 450 mm
- Path Width (W): 40 mm, and 80 mm
- Radius of Path Curvature (R): 100000 mm (approximate straight path), 250 mm, and 150 mm
- Frame Rate (F): 30 fps, 60 fps, 75 fps, 90 fps, 105 fps, 120 fps, 150 fps, and 180 fps

The final width (i.e., path width W) was calculated by adding twice the radius of the cursor ball to the diameter of the target ball ($path\ width = diameter\ of\ target\ ball + 2 \times radius\ of\ cursor\ ball$) [35]. It represented the maximum width a

cursor ball could push the target ball; that is, the cursor ball was right above or below the collided target ball (see Fig. 2. TOP). All conditions were evaluated in a pilot study. We ensured that there was no overlap between the start and end positions in each A, W, and R combination. Besides, an R of 100000 mm could be recognized as an approximate straight path.

As the refresh rate would impose an upper limit on the frame rate, our experiment was designed to maintain alignment between the refresh rate and the frame rate, thus allowing us to exercise control over the frame rates.

Specifically, we followed Wang et al.'s approach to control and build the frame rates in the experiments accurately [55]. We set the maximum frame rate and refresh rate through the NVIDIA control panel and Pimax control panel on the computer, respectively. In addition, we monitored the frame rates in both SteamVR and Unity, which collectively ensured the accuracy of the operating frame rates.

We applied two strategies to select the frame rate as our experimental conditions.

First, we chose six frame rates ranging from 30 fps to 180 fps with an interval of 30 fps. While 30 and 60 Hz might not be the dominant refresh rate for VR headsets, they are widely used in PC monitors; as such, participants would be familiar with them. We decided to include them because prior research had shown that the familiarity of frame rate could directly impact users' performance in immersive VEs with fast response task [55]. Concurrently, as evidenced in Fig. 1, the most commonly employed refresh rate for VR headsets is 90 Hz, serving as the predominant and most frequently encountered rate by VR HMD users.

The 120 Hz refresh rate has emerged as another popular option, with numerous new VR headsets incorporating this rate. Furthermore, 144 Hz is the prevailing refresh rate for high-refresh-rate PC displays, though it is currently infrequent for VR HMDs. However, to maintain consistent intervals between variables, we opted for 150 fps as our experimental condition. The current maximum refresh rate for VR headsets is 180 Hz, so an upper limit was also set for the frame rate in the experiments. Second, we further added 75 fps and 105 fps into our study; that is, the intermediates between 60 fps, 90 fps, and 120 fps. Wang et al. [55] found user performance at 90 fps was worse than at 60 fps and 120 fps in fast-response game-based scenarios. We wanted to explore whether a similar phenomenon occurs in fast-response tasks with more details. Thus, we included these two frame rates as our experimental conditions and had eight F conditions in total.

Given that frame rate (F) was our primary independent variable, the order of F was first counterbalanced across participants following a Latin Square approach. Within each F condition, the order of R was then counterbalanced across F conditions and participants. Finally, within each $F \times R$ condition, the order of $A \times W$ combination was randomly arranged and included five repetitions. This condition was simulated to reflect a scenario where participants consistently estimated F for each condition and responded to various steering paths with different complexities. In sum, a total of 17280 trials were recorded (3 $A \times 2$ $W \times 3$ $R \times 8$ $F \times 5$ repetitions $\times$ 24 participants).

The whole user study lasted about 50 minutes for each participant. We aimed to prevent potential distortions in the results caused by participant disengagement and fatigue in repetitive tasks [68]. Therefore, participants were instructed to take breaks between two F conditions until they were ready to proceed with the experiment. As a result, all participants consistently reported minimal or no fatigue throughout the user study.

Participants were first invited to complete a questionnaire to collect their demographic information. Subsequently, they were introduced to the VR device and the required task. Afterward, participants proceeded to wear the VR headset and initiate the practice trials, with the freedom to practice as many times as needed until they felt sufficiently prepared to commence the formal experiment (the training session took approximately five minutes). Once the participants were ready, they started to complete the formal trials. After participants completed all the experiments, we assessed their opinions and past experiences with each frame rate through an interview.

In summary, all the aforementioned approaches aimed to enhance the fidelity, reproducibility, and generalizability of the experiment by simulating real-application scenarios and evaluating users' behaviors in the VR steering tasks within varying frame rates.

4.5 Measurements

Three categories of data were logged after each trial, including movement time, success rate, and average movement speed.[3]

- **Movement Time** signifies the duration to accomplish a steering task from the start to the end position through the path. It has extensive application and modeling in various steering-based tasks [3, 35, 66].
- **Success Rate** is defined as the number of trials completed without interruptions (continuous contact between the cursor ball and the target ball) divided by the total number of trials.
- **Average Movement Speed** is the average speed at which a participant completes the whole steering task. Previous studies showed that the average movement speed is not synonymous with instantaneous speed (the speed at a specific path position) [47] but substantiated the approximation of the two for evaluation and modeling [26, 58, 66]. Therefore, in consonance with previous works, we also employed average movement speed as the metric in our study.

4.6 Results

We applied a two-step approach to remove outliers. First, we removed trials in which movement time exceeded 10 seconds. Through this process, 218 trials were removed (1.26% of total number of trials). Afterward, 224 trials (1.29%) that deviated by three times standard deviations from the averaged results in movement time and average movement speed were removed. In total, 442 data trials were removed from the results, representing 2.55% of the total trials.

We ran repeated-measures ANOVA (RM-ANOVA) tests to examine the three dependent variables. We used the Greenhouse-Geisser to adjust the degree of freedom if the assumption of sphericity is violated. Post-hoc pairwise comparisons were conducted using T-tests with Bonferroni corrections.

4.6.1 Movement Time

We found F ($F_{2.385,47.696} = 40.533, p < 0.001, \eta_p^2 = 0.670$), R ($F_{1.162,23.250} = 93.291, p < 0.001, \eta_p^2 = 0.823$), A ($F_{2,40} = 163.467, p < 0.001, \eta_p^2 = 0.891$) and W ($F_{1,20} = 401.332, p < 0.001, \eta_p^2 = 0.953$) had significant main effects on movement time. Additionally, significant interaction effects of $F \times R$ ($F_{5.948,118.958} = 6.460, p < 0.001, \eta_p^2 = 0.244$), $F \times W$ ($F_{4.393,87.853} = 5.649, p < 0.001, \eta_p^2 = 0.220$), $R \times A$ ($F_{2.225,44.498} = 11.468, p < 0.001, \eta_p^2 = 0.364$), $R \times W$ ($F_{2,40} = 15.245, p < 0.001, \eta_p^2 = 0.433$), and $A \times W$ ($F_{2,40} = 14.689, p < 0.001, \eta_p^2 = 0.423$) were found.

In terms of F, movement time at a 30 fps frame rate exhibited statistical significance by surpassing those at 60 fps (Δ (difference of means) $= 320ms$, $p = 0.005$), 75 fps ($\Delta = 503ms$, $p = 0.001$), 90 fps ($\Delta = 656ms$, $p < 0.001$), 105 fps ($\Delta = 749ms$, $p < 0.001$), 120 fps ($\Delta = 767ms$, $p < 0.001$), 150 fps ($\Delta = 787ms$, $p < 0.001$) and 180 fps ($\Delta = 766ms$, $p < 0.001$). Movement time at 60 fps was significantly longer than 90 fps ($\Delta = 335ms$, $p = 0.005$), 105 fps ($\Delta = 429ms$, $p < 0.001$), 120 fps ($\Delta = 446ms$, $p < 0.001$), 150 fps ($\Delta = 464ms$, $p < 0.001$) and 180 fps ($\Delta = 446s$, $p < 0.001$). The frame rate at 75 fps also showed a significantly longer movement time than 105 fps ($\Delta = 246ms$, $p = 0.001$), 120 fps ($\Delta = 263ms$, $p = 0.001$), 150 fps ($\Delta = 281ms$, $p < 0.001$) and 180 fps ($\Delta = 263s$, $p < 0.001$).

[3]To improve the readability, we do not use abbreviations MT and V for movement time and average movement speed in Sections 4.5 and 4.6, where we discuss the effects of frame rate and path characteristics. Please note that we use these abbreviations later in Section 5 for mathematical representations.

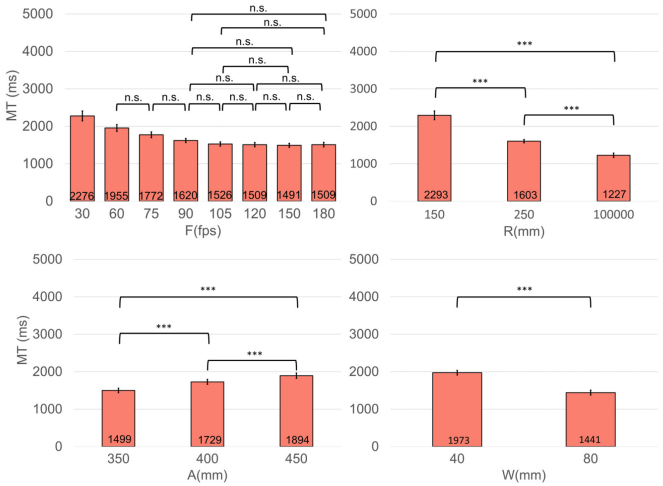

Fig. 3: Movement time (MT) for the variables that showed a significant main effect. The error bars show the standard errors. 'n.s.' and '***' indicate $p > 0.05$ and $p < 0.001$, respectively. All effects, excluding those indicated as 'n.s.', demonstrated statistical significance with a p-value less than 0.05 at least.

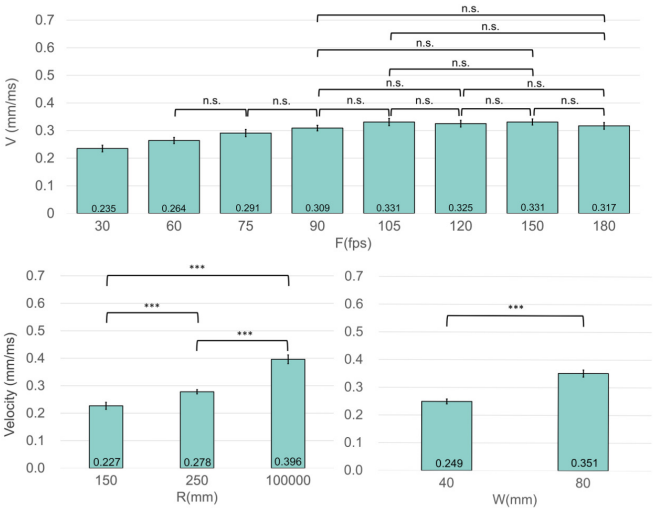

Fig. 4: Average movement speed for the variables that showed a significant main effect. The error bars show the standard error. '***' indicates $p < 0.001$. All effects, excluding those indicated as 'n.s.', demonstrated statistical significance with a p-value less than 0.05 at least.

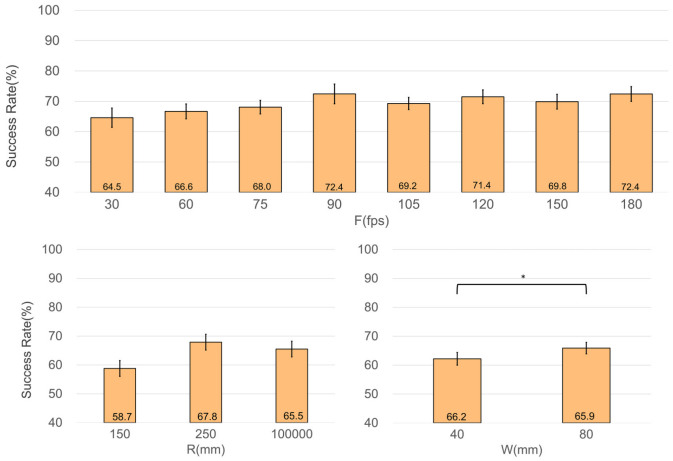

Fig. 5: Success rates for the variables that showed a significant main effect (except for R). The error bars show the standard errors. '*' indicates $p < 0.05$

In regard to factor R, significant variations are apparent among different conditions. Notably, when the R is 150 mm, the corresponding time expenditure significantly surpasses where the R is 250 mm ($\Delta = 690ms$, $p < 0.001$) or 100000 mm ($\Delta = 1066ms$, $p < 0.001$). Furthermore, for R equating to 250 mm, the time allocation demonstrates a significant elevation compared to instances when R is 100000 mm ($\Delta = 376ms$, $p < 0.001$). Within the factor A, the longest duration is observed at a length of 450 mm, which notably exceeds the movement time observed at lengths of 400 mm ($\Delta = 165ms$, $p < 0.001$) and 350 mm ($\Delta = 395ms$, $p < 0.001$). Moreover, a statistically significant distinction also exists between lengths of 400 mm and 350 mm ($\Delta = 230ms$, $p < 0.001$). Within W, a statistically significant increase in movement time was observed when the W was 40 mm, in contrast to the scenario where it was 80 mm ($\Delta = 532ms$, $p < 0.001$). These results were summarized in Fig. 3.

4.6.2 Success Rate

Results of RM-ANOVAs showed that F ($F_{7,140} = 2.831, p = 0.009, \eta_p^2 = 0.124$) and W ($F_{1,20} = 5.021, p = 0.037, \eta_p^2 = 0.201$) had significant main effects on success rate. Moreover, RM-ANOVA also revealed interaction effects of $R \times W$ ($F_{2,40} = 4.192, p < 0.024, \eta_p^2 = 0.173$) on success rate.

Although factor F demonstrated a significant main effect in the RM-ANOVA on success rate, post-hoc pairwise comparisons did not reveal a significant difference between different frame rates. Additionally, within the factor of W, a significant increase in success rate was observed when W equaled 80 mm in contrast to 40 mm ($\Delta = 3.8\%$, $p = 0.035$). The success rate results are shown in Fig. 5.

4.6.3 Average Movement Speed

RM-ANOVA revealed F ($F_{7,140} = 31.928, p < 0.001, \eta_p^2 = 0.615$), R ($F_{1.295,25.905} = 98.666, p < 0.001, \eta_p^2 = 0.831$) and W ($F_{1,20} = 295.834, p < 0.001, \eta_p^2 = 0.937$) had significant main effects on average movement speed. The significant interaction effects were found between $F \times R$ ($F_{14,280} = 1.848, p = 0.032, \eta_p^2 = 0.085$), and between $F \times W$ ($F_{7,140} = 3.008, p = 0.006, \eta_p^2 = 0.131$). R also revealed a significant interaction effect with A ($R \times A$: $F_{4,80} = 5.928, p < 0.001, \eta_p^2 = 0.229$), W ($W \times A$: $F_{1.336,26.727} = 24.815, p < 0.001, \eta_p^2 = 0.554$) and $A \times W$ ($R \times A \times W$: $F_{4,80} = 3.327, p = 0.026, \eta_p^2 = 0.143$). Moreover, RM-ANOVA results also showed interaction effects of $A \times W$ ($F_{2,40} = 4.571, p = 0.017, \eta_p^2 = 0.186$) on average movement speed.

The results of pairwise comparisons demonstrated that, at a F of 30 fps, the average movement speed significantly decreased in comparison to 60 fps ($\Delta = 0.029$, $p = 0.004$), 75 fps ($\Delta = 0.056$, $p < 0.001$), 90

fps ($\Delta = 0.075$, $p < 0.001$), 105 fps ($\Delta = 0.096$, $p < 0.001$), 120 fps ($\Delta = 0.090$, $p < 0.001$), 150 fps ($\Delta = 0.096$, $p < 0.001$), and 180 fps ($\Delta = 0.038$, $p < 0.001$). Furthermore, a statistically significant reduction in average movement speed was observed at 60 fps compared to 90 fps ($\Delta = 0.045$, $p = 0.002$), 105 fps ($\Delta = 0.067$, $p < 0.001$), 120 fps ($\Delta = 0.061$, $p < 0.001$), 150 fps ($\Delta = 0.066$, $p < 0.001$) and 180 fps ($\Delta = 0.053$, $p < 0.001$). This decrease was also observed at 75 fps compared to 105 fps ($\Delta = 0.040$, $p = 0.029$), 120 fps ($\Delta = 0.034$, $p = 0.013$), 150 fps ($\Delta = 0.039$, $p = 0.011$), 180 fps ($\Delta = 0.025$, $p = 0.04$).

In terms of factor R, when the R was set to 100000 mm, average movement speed exhibited a significant increase when contrasted with 250 mm ($\Delta = 0.118$, $p < 0.001$) and 150 mm ($\Delta = 0.169$, $p < 0.001$). Additionally, within factor W, a significant deceleration in average movement speed was revealed when W equaled 40 mm, as opposed to 80 mm ($\Delta = 0.102$, $p < 0.001$). These results are visualized in Fig. 4.

4.6.4 Subjective Feedback

In addition to the collected user behavior data, we conducted interviews with participants at the end of the experiment to gather their subjective insights and feelings about the interactions at different frame rates. Through the interview, participants reported that even though the order of frame rates was counterbalanced and the experimenter did not inform them about the frame rate used in each task, they were still able to perceive a distinct contrast between 30 fps, 60 fps, and higher frame rates. However, they could not discern differences between high frame rates, ranging from 90 fps to 180 fps. Some participants even suggested that there was no perceivable difference between two adjacent high frame rate conditions, such as 150 fps and 180 fps.

4.7 Discussion

4.7.1 Answers to RQ1: the Effects of Frame Fate on Steering Performance in Immersive VEs

Our results indicate a negative relationship between the F and movement time, suggesting that a higher frame rate is accompanied by a shorter completion time in the steering task in immersive VEs (see Fig. 3). This pattern is also reflected in the success rate, where a general trend emerges with higher F values corresponding to a higher success rate (see Fig. 5). The average movement speed follows the aforementioned trend, exhibiting significantly higher speeds as the frame rate increases (see Fig. 4).

In addition, our observations in the context of the steering task reveal a noteworthy pattern: once the frame rate exceeds 90 fps, no significant difference in performance metrics is demonstrated. This trend is in line with earlier studies proposing the notion of a threshold frame rate beyond which further improvements in user behavior are not discernible [55, 56]. Participants also reported similar subjective feelings in the interview. They could readily perceive the difference between low and high frame rates, but when the frame rate reached a certain threshold, they encountered difficulty in clearly distinguishing the difference between frame rates (see Sec. 4.6.4).

Moreover, it is important to note that while prior research has demonstrated the persistence of the phenomenon wherein higher frame rates continue to yield improved user performance even beyond 90 fps, these observations predominantly stem from the fast-paced scenario of shooting or action-oriented games [16, 18, 55]. Such contexts demand swift reactions within confined temporal intervals. The distinctive feature of our steering task lies in its lack of requirement for participants to execute rapid responses within abbreviated time frames. Instead, we emphasize a more naturalistic task engagement, wherein participants complete each trial without haste. In essence, within this non-fast-response task, a frame rate of 90 fps seems to be a discernible threshold, after which a further increase in frame rates may not provide additional significant improvements in participant behavior. In summary, tasks like the steering law, which do not require quick reactions compared to fast-paced gaming tasks, have a lower frame rate threshold to meet the demand [55].

Visual latency is one possible cause of the differences in the effects of frame rates on movement time (30–90 fps vs. 90–180 fps). We controlled the visual latency from the device and program (see Sec. 4.2.1) in our user study, leaving the frame rate the only source of visual latency. Prior work has shown that visual latency generated by different frame rates would result in different user perceptions of the moving target, thereby significantly impacting user performance in VEs [50, 52, 56]. In this work, when participants can perceive disparities in varying frame rates (lower than 90 fps), they might prefer to subjectively adapt their steering strategies to 'hedge' the visual lag caused by the low frame rate—they might slow down to align their control with the perceived velocity of the target. When participants cannot discern variations, particularly at frame rates exceeding 90 fps, they have similar behavior patterns in the steering task.

4.7.2 Answers to RQ2: the Effects of Path Features on Steering Performance

Within the factor R, our findings were consistent with previous research. A more curved path (a smaller R) leads to heightened task complexity, thereby prolonging movement time and lowering average movement speed [42, 66]. Regarding success rate, although no statistically significant difference was demonstrated, the condition with an R of 150 mm, representing the most curved path, exhibited the lowest success rate. Additionally, an R of 100000 mm, indicative of a nearly linear path, had a lower success rate compared to the 250 mm radius. One possible reason is that participants were more careful and spent greater cognitive effort when steering mildly curved paths.

Our investigation's results related to A and W substantiate prior observations [4, 62]. Specifically, the empirical outcomes affirm that narrower and shorter paths are concomitant with decreased movement time, improved success rate, and higher average movement speed. While A does not demonstrate statistically significant main effects on success rate and average movement speed, its observed trend remains consistently linear, the same as the expected impact of length on steering task performance.

5 Modeling and Fitting

In this section, our goals were fourfold: (1) verifying the applicability of steering law in immersive VR scenarios; (2) using a mathematical approach to summarize and generalize the effects of frame rates according to the results we got from the user study; (3) refining the original steering law model to improve the predictive accuracy of movement time (MT); (4) evaluating whether our two models have improved the predictive capability compared to current state-of-the-art models.

5.1 Verifying Steering Law's Applicability in Immersive VR Scenarios

We first checked the applicability of the original steering law [3] in immersive VR scenarios. Specifically, this validation involved assessing the prediction accuracy of MT across different path width and length pairs. The results were regressed between collected participants' performance MT and model prediction outcomes. Given that the original steering law model did not account for the effect of F and R on users' performance, we conducted separate analyses for each combination of F and R, with a total of 24 combinations ($8F \times 3R$). Within each $F \times R$ combination, there were 6 IDs ($3A \times 2W$). Finally, the original steering law shows excellent fits, as evidenced by the coefficient of determination r^2 for each $F \times R$ combination ($M = 0.969$, $SD = 0.07$).

5.2 Formulating the Effect of Frame Rate

We have empirically confirmed the effect of F on MT in the user study. In this section, we further examine the influence of F on MT through a quantitative modeling approach. To this end, we introduce the term F_{effect} to represent the impact of F.

Our statistical analysis demonstrates a main effect of F on MT (see Sec. 4.6.1). Therefore, we conducted regression analyses to fit the intricate relationship between F and MT at different conditions of F. Based on the results, MT initially decreases when F increases and stabilizes at a certain range when F reaches a specific threshold (see Sec. 4.7.1 & Sec. 8). Based on this trend, we explored four commonly used regression models: power, exponential, logarithmic, and

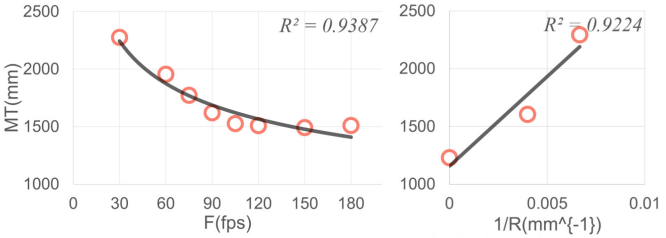

Fig. 6: Power regression of frame rate F on movement time MT ($N = 8$) (LEFT). Liner regression of $1/R$ on movement time MT ($N = 3$) (RIGHT).

second-order polynomial regression models. We calculated the coefficient of determination (r^2) to evaluate the fitted performance of the regression functions with respect to the results. The results revealed that the second-order polynomial function ($r^2 = 0.9899$) exhibited the best fit, followed by the power function ($r^2 = 0.9387$), logarithmic function ($r^2 = 0.9158$), and exponential function ($r^2 = 0.7877$). Despite the second-order polynomial function demonstrating the best performance, it involves more coefficients than others. It would lead to a complex model carrying the risk of overfitting, especially formulating the model with path features later on. On the other hand, the exponential function displayed the poorest fitting performance, suggesting an underfitting issue. A similar fitting performance was observed between the power function and logarithmic function. However, it is noteworthy that the overall trend of the logarithmic function does not align with our findings because MT turns negative when F exceeds a certain threshold, which could not happen. Thus, the power regression was finally chosen and conducted as shown in Fig. 6. LEFT. In the following sections, we denote this expression as $F_{effect}^{independent}$. The effect of F on MT can be formulated in Eq. (5).

$$F_{effect}^{independent} = MT = a(F)^b \tag{5}$$

Where a and b are empirical values from the regression. a is the coefficient and b is the exponent of the base F. The corresponding fitted values in our context are $a = 5429.4$ and $b = -0.26$. Thus, with the values of a and b in the equation, the trend we observed in the user study can be well formulated, i.e., the larger F is, the smaller MT is.

RM-ANOVA also revealed a main interaction effect of $F \times R$ and $F \times W$ on movement time. Like previous work [66], we incorporated the effects of $F \times R$ and $F \times W$ into the $F_{effect}^{independent}$ to represent the whole effect caused by F. Thus, the expression can be termed as $F_{effect}^{interaction}$. Moreover, considering the strong relationship on steering tasks between MT and $\frac{1}{R}$ that has been proven in both previous works [39, 66] and our results (see Figure 6. RIGHT), we replaced R by $\frac{1}{R}$ in the model as follows:

$$F_{effect}^{interaction} = MT = F_{effect}^{independent}(1 + \frac{1}{R} + W) \tag{6}$$

5.3 Models Formulation

From the F_{effect} results, we continue to refine the steering law and enhance the steering law's predictive and explanatory capabilities regarding MT in different conditions. In previous studies, no refined models included the effect of F in steering law. However, we found prior work has taken both effects of A, W, and R into account (refer to our discussion in Sec. 2.1). In light of this, we formulated and refined the model based on the most promising one (i.e., Eq. (4)) [66].

Based on the state-of-the-art model, further refinements were conducted to incorporate the F related effects. Following this prior research's approach, the factors that impact MT were added to the denominator of the original steering law [66]. Thus, we integrated $F_{effect}^{independent}$ into Eq. (4), resulting in the expression of **Candidate Model 1**:

$$\begin{aligned} MT &= a + b\frac{A}{W + c\frac{1}{R} + dW\frac{1}{R} + F_{effect}^{independent}} \\ &= a + b\frac{A}{W + c\frac{1}{R} + dW\frac{1}{R} + e(F)^f} \end{aligned} \tag{7}$$

Where values of $a - f$ represent empirical coefficients.

Using the same approach, we can also integrate $F_{effect}^{interaction}$ with Eq. (4) to derive **Candidate Model 2**:

$$\begin{aligned} MT &= a + b\frac{A}{W + c\frac{1}{R} + dW\frac{1}{R} + F_{effect}^{interaction}} \\ &= a + b\frac{A}{W + c\frac{1}{R} + dW\frac{1}{R} + F_{effect}^{R_{independent}}(1 + \frac{1}{R} + W)} \\ &= a + b\frac{A}{W + c\frac{1}{R} + dW\frac{1}{R} + e(F)^f + e\frac{1}{R}(F)^f + eW(F)^f} \end{aligned} \tag{8}$$

Where $a - f$ are empirical coefficients derived from regression evaluation.

5.4 Models Evaluation

5.4.1 Model Fitting Methods

In the process of fitting our nonlinear model, a nonlinear least squares optimization was conducted for estimating the parameters of the model [22]. Unlike linear models, the selection of initial values for the parameters plays a crucial role in navigating the parameter space effectively and finding the most accurate and reliable model fit. Given the model's complexity and the potential for multiple local minima, we adopted a randomized approach for the initial value selection. For each parameter, a wide range of potential values was defined (between -10 and 10), from which initial values were randomly generated. This process was iterated 1000 times, with each iteration involving a new set of random initial values for the model fitting. The effectiveness of each set of initial values was assessed based on the resulting R-squared value of the model fit, with the highest R-squared value indicating the most optimal fit. This iterative and randomized approach significantly enhanced the likelihood of identifying reliable and accurate parameter estimates for our model, albeit at the cost of increased computational effort.

5.4.2 Comparison Metrics

For completeness, the coefficient of determination (r^2) and the Akaike information criterion (AIC) were calculated to help us better understand and evaluate the models' performance. Here, r^2 signifies the predictive accuracy between predicted and observed MT (ranging from 0 to 1; the higher, the higher better). AIC is a quantitative measure used for model selection. It compares and evaluates different statistical models based on their goodness of fit and complexity [8]. Specifically, AIC aims to select the model that best represents the underlying relationship in the data while avoiding over-fitting, so it quantifies the trade-off between a model's fit to the data and the number of parameters it uses. AIC is calculated as $AIC = -2 * log - likelihood + 2 * number of parameters$, where $log - likelihood$ represents the maximized value of the log-likelihood function for the given model and dataset. The lower the AIC, the better the fitness of the candidate model.

5.4.3 Baseline Models

As demonstrated in Sec. 5.1, the applicability of the steering law with its transferability from 2D scenarios to immersive VEs is evident. Thus, we chose four of the most common and promising 2D-based steering models as our baseline (denoted as BL#): (BL1) the initial steering law model proposed by Accot and Zhai [3], (BL2) a refined version of the steering law model proposed by Nancel and Lank [42], which integrates the effect of curvature radius based on kinematics, and (BL3) and (BL4) are the refined models proposed by Yamanaka and Miyashita [66], which also consider the effects of curvature in the steering task, and

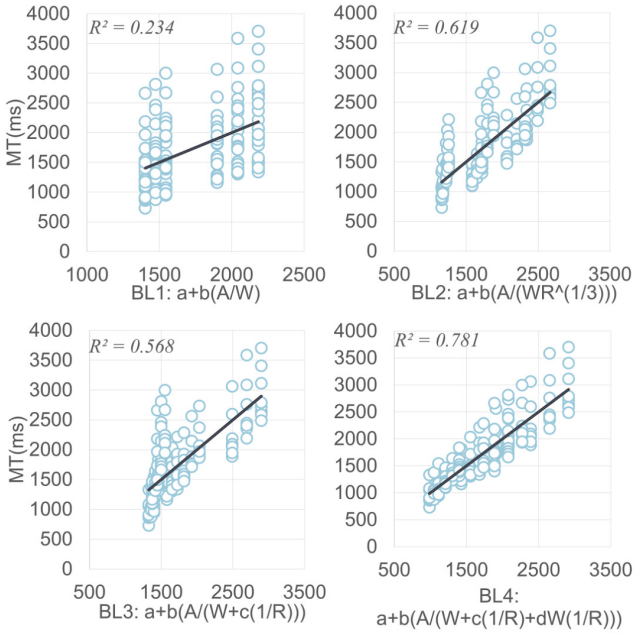

Fig. 7: Movement time (MT) model fitting across all conditions ($N = 90$) using the models from prior work [3, 42, 66].

Table 1: Models fitting results for predicting MT, including r^2 (where higher values indicate better fit) and AIC (where lower values indicate better performance) for models. r^2 and AIC in bold are the best values among them.

	Source	Model	r^2	AIC
BL1	[3]	$a+b\frac{W}{A}$	0.234	1815.72
BL2	[42]	$a+b\frac{A}{WR^{1/3}}$	0.618	1715.28
BL3	[66]	$a+b\frac{A}{W+c\frac{1}{R}}$	0.568	1733.14
BL4	[66]	$a+b\frac{A}{W+c\frac{1}{R}+dW\frac{1}{R}}$	0.781	1639.32
CM1	Candidate Model 1	$a+b\frac{A}{W+c\frac{1}{R}+dW\frac{1}{R}+F_{effect}^{independent}}$	**0.961**	**1386.46**
CM2	Candidate Model 2	$a+b\frac{A}{W+c\frac{1}{R}+dW\frac{1}{R}+F_{effect}^{interaction}}$	0.957	1397.84

(BL4) has the best performance in their work. These models are listed in Tab. 1 accordingly.

5.4.4 Result of Evaluation

We conducted nonlinear regression to fit the coefficients of each model and calculated the values of r^2 and AIC for comparison (values for coefficients in each model are listed in Tab. 3). Our results reveal that Candidate Model 1 (CM1) exhibits the best fitness (r^2 = 0.961, see Fig. 8. LEFT), closely followed by Candidate Model 2 (CM2, r^2 = 0.957, see Fig. 8. RIGHT). The third and fourth positions are held by Yamanaka and Miyashita's model with curvature-radius and width interactions (BL4, r^2 = 0.781) and Nancel and Lank's kinematic-based model (BL2, r^2 = 0.618), respectively (summarized in Fig. 7. RIGHT & MIDDLE-LEFT). Yamanaka and Miyashita's model, which did not consider the interaction effect, obtains an r^2 of 0.568 (BL3, see Fig. 7. MIDDLE-RIGHT). The result of the original steering law model received the lowest r^2 of 0.234 (BL1, see Fig. 7. LEFT). Regarding AIC, our candidate model CM1 demonstrates the optimal performance with a value of 1386.46, followed by CM2 (1397.84), BL4 (1639.32), BL2 (1715.28), BL3 (1733.14), and BL1 (1815.72).

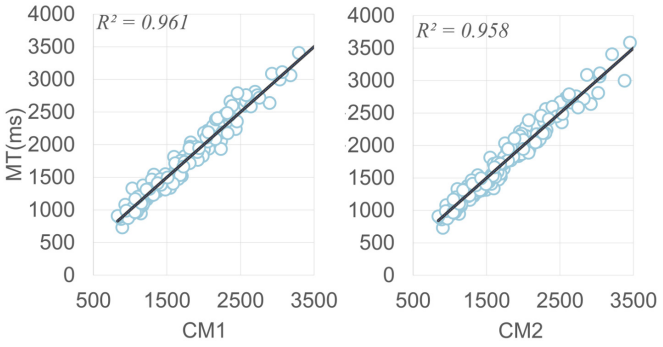

Fig. 8: Movement time (MT) model fitting across all conditions ($N = 90$) using the two proposed models.

5.5 Discussion

5.5.1 Answers to RQ3: Steering Law in Immersive VEs

Given that no prior work has verified the feasibility of the original steering law in immersive VR environments, we conducted empirical analyses to confirm the suitability before refining the original model. Since the model did not consider the factors of F and R, we analyzed each $F \times R$ combination independently to mitigate their effects. The fitness (r^2) for each pair on MT exhibited a high degree of performance ($M = 0.969$, $SD = 0.07$). This result strongly proves the applicability and extendability of the original steering law in immersive VR environments.

5.5.2 Answers to RQ4: Modeling Users' Behavior in Steering Tasks

We observed a main effect of F and an interaction effect of $F \times R$. The exponential regression was conducted to depict the general trend of MT at different F conditions. For the interaction effect, F, R, and W were formulated through multiplication. We termed these two expressions as $F_{effect}^{independent}$ and $F_{effect}^{interaction}$, as shown in Eq. (5) & Eq. (6). Then, the two F_{effect} were integrated in the current most promising model (see Eq. (7) & Eq. (8)). We demonstrated the proposed models' predictive accuracy compared to four baseline models. Both r^2 and AIC showed our models have the best predictive accuracy and performance.

Regarding the models we proposed, an interesting result is that the performance of the two proposed models is close to each other. Specifically, CM1 obtained the lowest AIC score ($\Delta = -11.38$, compared to CM2) and the highest r^2 ($\Delta = 0.004$, compared to CM2). This result could be attributed to two potential factors: (1) While the CM2 encompasses additional independent variables that may seem more explanatory, such as R and W, it may also introduce more noise, thereby diminishing the overall predictive power of the model. (2) There is a possibility that the optimal value was still not reached, although the initial values were chosen randomly. Nevertheless, it is important to note that this situation does not significantly impact our final results. Both models exhibit comparable performance, offering a superior explanation of user behavior compared to all the established baselines. Even with a modest improvement of 17.6%, our models underscore their effectiveness in capturing the intricacies of user behavior within different frame rates. Furthermore, CM1 and CM2 have the same number of coefficients, differing by only two more coefficients when compared to the baselines, which did not take the effect F into account. The 6 coefficients in our current model account for the more complex scenario when the path is curved, allowing us to represent different task difficulties. However, if we restrict our consideration to cases where the path is straight, as in previous work, we only have four coefficients written as $MT = a + b\frac{A}{W+c(F)^d}$. The number of coefficients equals the previously enhanced steering law model [62, 66]. Moreover, the values of coefficients, e and f, after being regressed from our models, accurately describe and present the trend we observed in the user study,

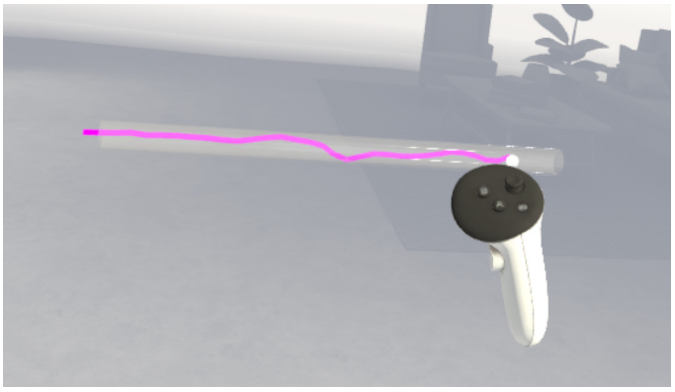

Fig. 9: A screenshot of the application scenario. The white semi-transparent tunnel is the path to be traced by the participants. The white sphere on the controller serves as the cursor (i.e., the brush nib), while the pink line represents the line drawn by the participant.

where a larger F leads to a smaller MT (see Tab. 3).

In summary, we consider that the performance of our two proposed models is best; both models maintain simplicity, and all the coefficients are interpretable, avoiding the risk of overfitting. Moreover, the two models demonstrated strong applicability across various difficult tasks that are represented by R within our experimental settings. Therefore, these results imply that for accurately establishing steering law across various conditions ($A \times W \times R \times F$), it necessarily needs to consider the factors F.

6 Example Application

We aimed to investigate the applicability and generalizability of our proposed models further. To achieve this, we selected a tracing task—to simulate authentic VR-based painting activities, where users typically utilize a controller as a brush to draw their intended or pre-designed patterns within VEs [11]. We conducted a second user study to collect user steering performance in this tracing task under different conditions and introduced a new application scenario. Using the collected behavior data, we first applied the proposed models and the model from prior work to predict both movement time (MT) and average movement speed (V), and then compared the discrepancies between the predicted and observed values.

6.1 Participants, Apparatus, and Task

Fifteen participants were recruited in this study (8 females and 7 males, aged between 19 and 25, M = 21.9, SD = 2.53). None of them participated in the first study. Six participants had prior experience with VR HMDs. All of them reported they were able to see all the virtual objects in the headset.

In this study, we used a Meta Quest 3 VR headset. This device features a 2064×2208 per eye resolution screen, a maximum refresh rate of 120Hz, and a FoV of 110 degrees horizontally and 96 degrees vertically. The experimental program was developed using the Unity3D game engine with C# and integrated with the Oculus Interaction SDK (version 57.0.2). This program was developed and run on a computer with the same configurations as in the first study.

In our study, we developed a tracing task using a predefined semi-translucent tunnel as the path for participants to follow. This tunnel was configured with three conditions: width, length, and curvature. Within each trial, participants needed to hold the controller with a small sphere affixed to the top, which served as the cursor to indicate where the line would be rendered. Once ready for a trial, they pressed and held the trigger button and navigated the cursor through the tunnel to draw a replicated pattern. The steering duration was measured from the moment the sphere entered the tunnel until it exited. Notably, only successful trials were recorded. If the cursor sphere crossed the tunnel boundary, participants were required to restart the trial.

Table 2: Models fitting results for predicting MT and V, including r^2 (where higher values indicate better fit) and AIC (where lower values indicate better performance) for models. r^2 and AIC in bold are the best across models.

Source	MT		V	
	r^2	AIC	r^2	AIC
Baseline	0.813	624.5	0.739	-342.6
$model_{independent}$	**0.935**	**565.2**	**0.857**	**-370.82**
$model_{interaction}$	0.927	571.9	0.854	-370.1

6.2 Design and Procedure

A within-subjects design was used in this study with four within-subjects factors, including 3 frame rates F (30 fps, 75 fps, and 90 fps), 3 path lengths A, 2 path widths W, and 3 curvature radii R. To increase comparability, we kept the conditions in A, W, and R with the same values as in the first user study. As in our proposed models, only the effects of F were integrated into the outperformed model from prior work that has included the effects of A, W, and R [66]. Therefore, the variations of A, W, and R would not affect our models' performance.

Regarding the values of F, we initially aimed to simulate user behavior at the most commonly used or default frame rates in VR headsets (see Figure 1). To provide a comprehensive analysis, we also considered users' performance under low frame rate conditions, which are frequently encountered in real applications, as discussed in Section 2.3. Given that the maximum refresh rate of Meta Quest 3 is 120 Hz, we selected three frame rates for this study: 90 fps (*commonly used*), 75 fps (*intermediate*), and 30 fps (*low frame rate*).

The experimental procedure and the order of the within-subjects factor conditions were the same as in the first user study, as described in Section 4. The whole duration of the experiment was approximately 15 minutes for each participant. In total, we collected $3F \times 3A \times 2W \times 3R \times$ 5 repetitions $\times$ 15 participants = 4050 data trials in this study.

6.3 Predicting Average Movement Time

We pre-processed the data in the same way as in the first study. In total, we removed 72 trials, which accounts for 1.77% of the total number of trials.

To demonstrate the capabilities of our models, we used the current most promising model, the same as the baseline in the first user study (see Eq. (4)). For simplicity, We rename the Candidate Models 1 and 2 as $model_{independent}$ and $model_{interaction}$, respectively, according to their attributes in terms of the F_{effect}. Tab. 2 summarizes the results. The baseline model showed the worst performance across all metrics. The results revealed that the $model_{independent}$ was still the best predictive performance across all conditions. This outcome is consistent with our conclusion in Sec. 5.4.

6.4 Predicting Average Movement Speed

Based on previous work, the average time equals the moving distance divided by the average velocity. We present our denominator separately for predicting the average movement speed V [26, 39, 66]. The $model_{independent}$ and $model_{interaction}$ can be expressed as:

$$V = a + bW + c\frac{1}{R} + dW\frac{1}{R} + F_{effect}^{independent} \tag{9}$$

$$V = a + bW + c\frac{1}{R} + dW\frac{1}{R} + F_{effect}^{interaction} \tag{10}$$

The baseline model can be expressed as:

$$V = a + bW + c\frac{1}{R} + dW\frac{1}{R} \tag{11}$$

We used these models to predict the V we obtained from the experiment to examine our models further. Same as in the prediction of movement time, $Model_{independent}$ has the highest predictive accuracy, then the second highest prediction rate is $model_{interaction}$, and the

worst is the baseline. Finally, AIC results show that $model_{independent}$ performs optimally with our studies.

7 Summary of Findings and Recommendations

In this section, we briefly summarize the main findings of this work, accompanied by pertinent recommendations.

In the user study (Sec. 4), the dataset encompassing various conditions (A, W, R, and F) was collected and evaluated in terms of movement time, success rate, and average movement speed. Our results discovered the impact of F on user behavior and performance, unveiling the direct effect of F on user performance. Furthermore, we identified a threshold at 90 fps, beyond which frame rates did not significantly improve performance in a non-fast-response task. Moreover, our study confirmed the consistency of observed trends in path characteristics (A, W, and R) with prior research and validated the possibility of applying and modeling steering law to immersive VR scenarios.

Based on the results from the user study, we verified the applicability of steering law in immersive VR environments, which shows strong fits ($M = 0.969$, $SD = 0.07$). Two models (see CM1 and CM2 in Sec. 5) were then built by formulating the effects of frame rate and integrating them into the current most promising model. We found the proposed models achieved high prediction accuracy for predicting MT (r^2 exceeds 0.957 for both models). The prediction accuracy shows improvements of at least 17.6% compared to past models. Moreover, they have exhibited a remarkable 72.7% enhancement in r^2 and a notable 23.6% improvement in AIC compared to the original steering law model.

Furthermore, we demonstrated the usefulness of the proposed models in Sec. 6. We applied the proposed models to predict movement time and average movement speed. To verify their robustness and reproducibility, we conducted a follow-up user study with a tracing task using the three most typical frame rates to collect user performance. The two proposed models show the best predictive accuracy on both movement time and average movement speed (see Tab. 2).

Finally, we prove that in immersive VR, the frame rate can directly affect human behavior and performance, even for tasks where users do not need to react within a short period of time. Thus, combined with previous VR-based gaming tasks [55], it is possible to conclude that frame rate would affect participant behavior regardless of whether its task demands the user to respond within a limited period of time or not. Moreover, we found that increasing the frame rate does not significantly affect the user's behavior further after reaching a certain threshold (90 fps in our case and 120 fps in the gaming-based task). Therefore, based on our findings, we make two recommendations: (1) while different tasks have varying thresholds for frame rate, for better standardization, 90 fps would be optimized to use as the minimum lower frame rate threshold with non-fast-response tasks and 120 fps serves as the minimum frame threshold for fast-response tasks when the device is available [55]. (2) To enhance reproducibility in future VR research, researchers should explicitly report the frame rates and device refresh rates employed in human-computer interaction experiments when detailing study specifics.

8 Limitations and Future Work

According to our current work, four main limitations were identified and represent possible avenues for future research.

First, we found that user behavior was not significantly affected by high frame rates (from 90 fps to 180 fps). However, considering the limitation of the maximum refresh rate of current devices, we cannot evaluate effects with frame rates higher than 180 fps in VR headsets. In addition, since we employed the exponential regression to construct the F_{effect}, we recommend applying our models for predicting MT and V within the range of 30-180 fps when using it. However, it is worth noting that the frame rate intervals chosen in our studies already encompass all the current common frame rates in today's VR headsets. In the future, as devices with higher refresh rates become accessible, it is essential to investigate and verify whether user behavior remains unaffected at these elevated refresh rates.

Second, our experimental design only asked participants to steer in one direction—from left to right. Though it is a standard approach applied in prior studies either in 2D contexts [3, 62, 64–66] or 3D environments [35], we believe it may also be worthwhile to investigate the effect of steering direction in the future, given that users have more freedom in interacting with immersive VR environments.

Third, we demonstrated the effectiveness of frame rate across varying path lengths and widths in our studies. However, we used 8 frame rates as our within-subject conditions, which resulted in numerous repetitive steering times and extended experimental duration. To mitigate potential participant impatience and disengagement [68], we limited our investigations to 3 path widths and 2 path lengths. Therefore, we intend to explore more complex scenarios in the future by examining additional path features and verifying our results and models in more application scenes.

Finally, our research employed the steering law, a standard non-fast-response task, to evaluate user behavioral patterns across varying frame rates. While our findings indicate no significant variance in user behavioral performance once the frame rate surpasses a certain threshold (90 fps), it is important to acknowledge potential discrepancies across diverse tasks. For instance, more intricate interaction scenarios and tasks might yield different threshold outcomes compared to those identified in our study. Therefore, in the future, we intend to systematically analyze the thresholds under various interaction scenarios and explore potential patterns between these thresholds and interaction characteristics.

9 Conclusion

In this work, we investigated the effects of frame rate and path configurations (length, width, and radius of curvature) on steering task performance in virtual reality (VR) head-mounted displays (HMDs) through a user study. Based on the results, we proposed two models for predicting steering movement time and average movement speed. Our work shows that our models, which consider the effects of VR HMDs' frame rate, achieved better prediction performance than the existing models. To further evaluate the robustness of the proposed models, we applied them in a tracing task to predict the users' performance and compared the prediction results with user behavior data collected. The results of this evaluation show that the two models can achieve high prediction performance. Our findings can help understand and predict steering actions, such as navigating through menus or drawing lines, thereby supporting decision-making in interaction design for VR HMDs. Furthermore, our results bridge the gap between the effects of frame rate on user behavior in non-fast-response tasks and confirm the necessity of reporting device refresh rates and frame rates in future human-computer interaction experiments using VR HMDs.

References

[1] MonoBehaviour.Update - Unity Scripting API. https://docs.unity3d.com/ScriptReference/MonoBehaviour.Update.html, 2024. Accessed: 2024-03-26. 4

[2] SteamVR Tracking - Valve Partner Website. https://partner.steamgames.com/vrlicensing, 2024. Accessed: 2024-03-26. 4

[3] J. Accot and S. Zhai. Beyond fitts' law: Models for trajectory-based hci tasks. In *Proceedings of the ACM SIGCHI Conference on Human Factors in Computing Systems*, CHI '97, p. 295–302. Association for Computing Machinery, New York, NY, USA, 1997. doi: 10.1145/258549.258760 1, 2, 3, 5, 7, 8, 9, 11

[4] J. Accot and S. Zhai. Performance evaluation of input devices in trajectory-based tasks: An application of the steering law. In *Proceedings of the SIGCHI Conference on Human Factors in Computing Systems*, CHI '99, p. 466–472. Association for Computing Machinery, New York, NY, USA, 1999. doi: 10.1145/302979.303133 3, 7

[5] J. Accot and S. Zhai. Scale effects in steering law tasks. In *Proceedings of the SIGCHI Conference on Human Factors in Computing Systems*, CHI '01, p. 1–8. Association for Computing Machinery, New York, NY, USA, 2001. doi: 10.1145/365024.365027 3

[6] D. Ahlström. Modeling and improving selection in cascading pull-down menus using fitts' law, the steering law and force fields. In *Proceedings of the SIGCHI Conference on Human Factors in Computing Systems*, CHI

'05, p. 61–70. Association for Computing Machinery, New York, NY, USA, 2005. doi: 10.1145/1054972.1054982 3

[7] J. M. Airey, J. H. Rohlf, and F. P. Brooks. Towards image realism with interactive update rates in complex virtual building environments. *SIGGRAPH Comput. Graph.*, 24(2):41–50, feb 1990. doi: 10.1145/91394.91416 3

[8] H. Akaike. A new look at the statistical model identification. *IEEE Transactions on Automatic Control*, 19(6):716–723, 1974. doi: 10.1109/TAC.1974.1100705 8

[9] R. Balakrishnan. "beating" fitts' law: Virtual enhancements for pointing facilitation. *Int. J. Hum.-Comput. Stud.*, 61(6):857–874, dec 2004. doi: 10.1016/j.ijhcs.2004.09.002 2

[10] R. C. A. Barrett, R. Poe, J. W. O'Camb, C. Woodruff, S. M. Harrison, K. Dolguikh, C. Chuong, A. D. Klassen, R. Zhang, R. B. Joseph, et al. Comparing virtual reality, desktop-based 3d, and 2d versions of a category learning experiment. *Plos one*, 17(10):e0275119, 2022. doi: 10.1371/journal.pone.0275119 3

[11] W. Bolier, W. Hürst, G. van Bommel, J. Bosman, and H. Bosman. Drawing in a virtual 3d space - introducing vr drawing in elementary school art education. In *Proceedings of the 26th ACM International Conference on Multimedia*, MM '18, p. 337–345. Association for Computing Machinery, New York, NY, USA, 2018. doi: 10.1145/3240508.3240692 10

[12] R. Brown. Vrcompare website. https://vr-compare.com/, 2023. 2

[13] S. T. Bryson. Effects of lag and frame rate on various tracking tasks. In *Stereoscopic Displays and Applications IV*, vol. 1915, pp. 155–166. SPIE, 1993. doi: 10.1117/12.157034 3

[14] J. Y. C. Chen and J. E. Thropp. Review of low frame rate effects on human performance. *IEEE Transactions on Systems, Man, and Cybernetics - Part A: Systems and Humans*, 37(6):1063–1076, 2007. doi: 10.1109/TSMCA.2007.904779 3

[15] J. W. Choi, B. H. Kim, S. Huh, and S. Jo. Observing actions through immersive virtual reality enhances motor imagery training. *IEEE Transactions on Neural Systems and Rehabilitation Engineering*, 28(7):1614–1622, 2020. doi: 10.1109/TNSRE.2020.2998123 3

[16] K. T. Claypool and M. Claypool. On frame rate and player performance in first person shooter games. *Multimedia systems*, 13(1):3–17, 2007. doi: 10.1007/s00530-007-0081-1 3, 7

[17] M. Claypool and K. Claypool. Perspectives, frame rates and resolutions: It's all in the game. In *Proceedings of the 4th International Conference on Foundations of Digital Games*, FDG '09, p. 42–49. Association for Computing Machinery, New York, NY, USA, 2009. doi: 10.1145/1536513.1536530 1, 3

[18] M. Claypool, K. Claypool, and F. Damaa. The effects of frame rate and resolution on users playing first person shooter games. In S. Chandra and C. Griwodz, eds., *Multimedia Computing and Networking 2006*, vol. 6071, p. 607101. International Society for Optics and Photonics, SPIE, 2006. doi: 10.1117/12.648609 3, 7

[19] J. Davis, Y.-H. Hsieh, and H.-C. Lee. Humans perceive flicker artifacts at 500 hz. *Scientific reports*, 5(1):7861, 2015. doi: 10.1038/srep07861 3

[20] J. T. Dennerlein, D. B. Martin, and C. Hasser. Force-feedback improves performance for steering and combined steering-targeting tasks. In *Proceedings of the SIGCHI Conference on Human Factors in Computing Systems*, CHI '00, p. 423–429. Association for Computing Machinery, New York, NY, USA, 2000. doi: 10.1145/332040.332469 3

[21] B. Duinkharjav, P. Chakravarthula, R. Brown, A. Patney, and Q. Sun. Image features influence reaction time: A learned probabilistic perceptual model for saccade latency. *ACM Trans. Graph.*, 41(4), jul 2022. doi: 10.1145/3528223.3530055 3

[22] J. Eriksson. *Optimization and regularization of nonlinear least squares problems*. Verlag nicht ermittelbar Jerusalem, 1996. 8

[23] P. M. Fitts. The information capacity of the human motor system in controlling the amplitude of movement. *Journal of experimental psychology*, 47(6):381, 1954. 2

[24] T. Flash and N. Hogan. The coordination of arm movements: an experimentally confirmed mathematical model. *Journal of neuroscience*, 5(7):1688–1703, 1985. 2

[25] S. Hauswiesner, D. Kalkofen, and D. Schmalstieg. Multi-frame rate volume rendering. In *Proceedings of the 10th Eurographics Conference on Parallel Graphics and Visualization*, EG PGV'10, p. 19–26. Eurographics Association, Goslar, DEU, 2010. 3

[26] E. R. Hoffmann. Review of models for restricted-path movements. *International Journal of Industrial Ergonomics*, 39(4):578–589, 2009. Special issue: Felicitating Colin G. Drury. doi: 10.1016/j.ergon.2008.02.007 5, 10

[27] W. Hürst and M. Helder. Mobile 3d graphics and virtual reality interaction. In *Proceedings of the 8th International Conference on Advances in Computer Entertainment Technology*, ACE '11. Association for Computing Machinery, New York, NY, USA, 2011. doi: 10.1145/2071423.2071458 1

[28] S. Kavanagh, A. Luxton-Reilly, B. Wuensche, and B. Plimmer. A systematic review of virtual reality in education. *Themes in Science and Technology Education*, 10(2):85–119, 2017. 1

[29] E. M. Kolasinski. Simulator sickness in virtual environments. 1995. 3

[30] R. Kumar, V. V. Phoha, and A. Serwadda. Continuous authentication of smartphone users by fusing typing, swiping, and phone movement patterns. In *2016 IEEE 8th international conference on biometrics theory, applications and systems (BTAS)*, pp. 1–8. IEEE, 2016. doi: 10.1109/BTAS.2016.7791164 1

[31] F. Lacquaniti, C. Terzuolo, and P. Viviani. The law relating the kinematic and figural aspects of drawing movements. *Acta Psychologica*, 54(1):115–130, 1983. doi: 10.1016/0001-6918(83)90027-6 2

[32] B. S. Lange, P. Requejo, S. M. Flynn, A. A. Rizzo, F. Valero-Cuevas, L. Baker, and C. Winstein. The potential of virtual reality and gaming to assist successful aging with disability. *Physical Medicine and Rehabilitation Clinics*, 21(2):339–356, 2010. doi: 10.1016/j.pmr.2009.12.007 1

[33] D. S. Leibowitz. *Mobile Digital Art: Using the IPad and IPhone as Creative Tools*. Taylor & Francis, 2013. 1

[34] L. Li, F. Yu, D. Shi, J. Shi, Z. Tian, J. Yang, X. Wang, and Q. Jiang. Application of virtual reality technology in clinical medicine. *American journal of translational research*, 9(9):3867, 2017. 1

[35] L. Liu, J.-B. Martens, and R. van Liere. Revisiting path steering for 3d manipulation tasks. In *2010 IEEE Symposium on 3D User Interfaces (3DUI)*, pp. 39–46, 2010. doi: 10.1109/3DUI.2010.5444724 2, 3, 4, 5, 11

[36] I. S. MacKenzie. Fitts' law as a research and design tool in human-computer interaction. *Hum.-Comput. Interact.*, 7(1):91–139, mar 1992. doi: 10.1207/s15327051hci0701_3 2

[37] I. S. MacKenzie and C. Ware. Lag as a determinant of human performance in interactive systems. In *Proceedings of the INTERACT '93 and CHI '93 Conference on Human Factors in Computing Systems*, CHI '93, p. 488–493. Association for Computing Machinery, New York, NY, USA, 1993. doi: 10.1145/169059.169431 3

[38] M. Menozzi, F. Lang, U. Näpflin, C. Zeller, and H. Krueger. Crt versus lcd: effects of refresh rate, display technology and background luminance in visual performance. *Displays*, 22(3):79–85, 2001. doi: 10.1016/S0141-9382(01)00054-3 1

[39] M. Montazer, C. Drury, and M. Karwan. An optimization model for self-paced tracking on circular courses. *IEEE Transactions on Systems, Man, and Cybernetics*, 18(6):908–916, 1988. doi: 10.1109/21.23090 2, 8, 10

[40] D. Monteiro, H.-N. Liang, J. Wang, H. Chen, and N. Baghaei. An in-depth exploration of the effect of 2d/3d views and controller types on first person shooter games in virtual reality. In *2020 IEEE International Symposium on Mixed and Augmented Reality (ISMAR)*, pp. 713–724, 2020. doi: 10.1109/ISMAR50242.2020.00102 3

[41] P. Monteiro, D. Carvalho, M. Melo, F. Branco, and M. Bessa. Application of the steering law to virtual reality walking navigation interfaces. *Computers & Graphics*, 77:80–87, 2018. doi: 10.1016/j.cag.2018.10.003 3, 4

[42] M. Nancel and E. Lank. Modeling user performance on curved constrained paths. In *Proceedings of the 2017 CHI Conference on Human Factors in Computing Systems*, CHI '17, p. 244–254. Association for Computing Machinery, New York, NY, USA, 2017. doi: 10.1145/3025453.3025951 2, 3, 7, 8, 9

[43] R. Pausch. Virtual reality on five dollars a day. In *Proceedings of the SIGCHI Conference on Human Factors in Computing Systems*, CHI '91, p. 265–270. Association for Computing Machinery, New York, NY, USA, 1991. doi: 10.1145/108844.108913 3

[44] A. N. Ramaseri Chandra, F. El Jamiy, and H. Reza. A systematic survey on cybersickness in virtual environments. *Computers*, 11(4), 2022. doi: 10.3390/computers11040051 2

[45] D. Saredakis, A. Szpak, B. Birckhead, H. A. Keage, A. Rizzo, and T. Loetscher. Factors associated with virtual reality sickness in head-mounted displays: a systematic review and meta-analysis. *Frontiers in human neuroscience*, 14:96, 2020. doi: 10.3389/fnhum.2020.00096 1

[46] R. Senanayake and R. S. Goonetilleke. Pointing device performance in steering tasks. *Perceptual and Motor Skills*, 122(3):886–910, 2016. PMID: 27216944. doi: 10.1177/0031512516649717 3

[47] R. Senanayake, E. R. Hoffmann, and R. S. Goonetilleke. A model for combined targeting and tracking tasks in computer applications. *Experimental brain research*, 231:367–379, 2013. doi: 10.1007/s00221-013-3700-4 5

[48] N. E. Seymour, A. G. Gallagher, S. A. Roman, M. K. O'brien, V. K. Bansal, D. K. Andersen, and R. M. Satava. Virtual reality training improves operating room performance: results of a randomized, double-blinded study. *Annals of surgery*, 236(4):458, 2002. doi: 10.1097/00000658-200210000-00008 1

[49] M. Shahzad, A. X. Liu, and A. Samuel. Secure unlocking of mobile touch screen devices by simple gestures: You can see it but you can not do it. In *Proceedings of the 19th Annual International Conference on Mobile Computing & Networking*, MobiCom '13, p. 39–50. Association for Computing Machinery, New York, NY, USA, 2013. doi: 10.1145/2500423.2500434 1

[50] J. Spjut, B. Boudaoud, K. Binaee, J. Kim, A. Majercik, M. McGuire, D. Luebke, and J. Kim. Latency of 30 ms benefits first person targeting tasks more than refresh rate above 60 hz. In *SIGGRAPH Asia 2019 Technical Briefs*, SA '19, p. 110–113. Association for Computing Machinery, New York, NY, USA, 2019. doi: 10.1145/3355088.3365170 3, 4, 7

[51] G. Székely and R. M. Satava. Virtual reality in medicine. *BMJ: British Medical Journal*, 319(7220):1305, 1999. 1

[52] V. van Polanen, R. Tibold, A. Nuruki, and M. Davare. Visual delay affects force scaling and weight perception during object lifting in virtual reality. *Journal of neurophysiology*, 121(4):1398–1409, 2019. 7

[53] P. Viviani and T. Flash. Minimum-jerk, two-thirds power law, and isochrony: converging approaches to movement planning. *Journal of Experimental Psychology: Human Perception and Performance*, 21(1):32, 1995. 2

[54] J. Wang, R. Shi, Z. Xiao, X. Qin, and H.-N. Liang. Effect of render resolution on gameplay experience, performance, and simulator sickness in virtual reality games. *Proc. ACM Comput. Graph. Interact. Tech.*, 5(1), may 2022. doi: 10.1145/3522610 3

[55] J. Wang, R. Shi, W. Zheng, W. Xie, D. Kao, and H.-N. Liang. Effect of frame rate on user experience, performance, and simulator sickness in virtual reality. *IEEE Transactions on Visualization and Computer Graphics*, 29(5):2478–2488, 2023. doi: 10.1109/TVCG.2023.3247057 1, 2, 3, 4, 5, 7, 11

[56] C. Ware and R. Balakrishnan. Reaching for objects in vr displays: Lag and frame rate. *ACM Trans. Comput.-Hum. Interact.*, 1(4):331–356, dec 1994. doi: 10.1145/198425.198426 1, 3, 7

[57] B. Watson, V. Spaulding, N. Walker, and W. Ribarsky. Evaluation of the effects of frame time variation on vr task performance. In *Proceedings of IEEE 1997 Annual International Symposium on Virtual Reality*, pp. 38–44, 1997. doi: 10.1109/VRAIS.1997.583042 3

[58] B. Watson, N. Walker, W. Ribarsky, and V. Spaulding. Effects of variation in system responsiveness on user performance in virtual environments. *Human Factors*, 40(3):403–414, 1998. 3, 5

[59] F. Weidner, A. Hoesch, S. Poeschl, and W. Broll. Comparing vr and non-vr driving simulations: An experimental user study. In *2017 IEEE Virtual Reality (VR)*, pp. 281–282, 2017. doi: 10.1109/VR.2017.7892286 3

[60] D. Wolf, J. J. Dudley, and P. O. Kristensson. Performance envelopes of in-air direct and smartwatch indirect control for head-mounted augmented reality. In *2018 IEEE Conference on Virtual Reality and 3D User Interfaces (VR)*, pp. 347–354, 2018. doi: 10.1109/VR.2018.8448289 3, 4

[61] B. Xie, H. Liu, R. Alghofaili, Y. Zhang, Y. Jiang, F. D. Lobo, C. Li, W. Li, H. Huang, M. Akdere, et al. A review on virtual reality skill training applications. *Frontiers in Virtual Reality*, 2:645153, 2021. doi: 10.3389/frvir.2021.645153 1

[62] S. Yamanaka. Steering performance with error-accepting delays. In *Proceedings of the 2019 CHI Conference on Human Factors in Computing Systems*, CHI '19, p. 1–9. Association for Computing Machinery, New York, NY, USA, 2019. doi: 10.1145/3290605.3300800 1, 4, 7, 9, 11

[63] S. Yamanaka, T. Kinoshita, Y. Oba, R. Tomihari, and H. Miyashita. Varying subjective speed-accuracy biases to evaluate the generalizability of experimental conclusions on pointing-facilitation techniques. In *Proceedings of the 2023 CHI Conference on Human Factors in Computing Systems*, CHI '23. Association for Computing Machinery, New York, NY, USA, 2023. doi: 10.1145/3544548.3580740 2

[64] S. Yamanaka and H. Miyashita. Modeling the steering time difference between narrowing and widening tunnels. In *Proceedings of the 2016 CHI Conference on Human Factors in Computing Systems*, CHI '16, p. 1846–1856. Association for Computing Machinery, New York, NY, USA, 2016. doi: 10.1145/2858036.2858037 11

[65] S. Yamanaka and H. Miyashita. Scale effects in the steering time difference between narrowing and widening linear tunnels. In *Proceedings of the 9th Nordic Conference on Human-Computer Interaction*, NordiCHI '16. Association for Computing Machinery, New York, NY, USA, 2016. doi: 10.1145/2971485.2971486 11

[66] S. Yamanaka and H. Miyashita. Modeling pen steering performance in a single constant-width curved path. In *Proceedings of the 2019 ACM International Conference on Interactive Surfaces and Spaces*, ISS '19, p. 65–76. Association for Computing Machinery, New York, NY, USA, 2019. doi: 10.1145/3343055.3359697 1, 2, 4, 5, 7, 8, 9, 10, 11

[67] Z. Yin and J. R. Mourant. The perception of optical flow in driving simulators. In *Driving Assesment Conference*, pp. 176–182. University of Iowa, 2009. 3

[68] D. Yu, Q. Zhou, B. Tag, T. Dingler, E. Velloso, and J. Goncalves. Engaging participants during selection studies in virtual reality. In *2020 IEEE Conference on Virtual Reality and 3D User Interfaces (VR)*, pp. 500–509, 2020. doi: 10.1109/VR46266.2020.00071 2, 5, 11

[69] S. Zhai, J. Accot, and R. Woltjer. Human action laws in electronic virtual worlds: An empirical study of path steering performance in vr. *Presence*, 13(2):113–127, 2004. doi: 10.1162/1054746041382393 3

[70] L. Zhao, T. Isenberg, F. Xie, H.-N. Liang, and L. Yu. Metacast: Target-and context-aware spatial selection in vr. *arXiv preprint arXiv:2308.03616*, 2023. 1

[71] X. Zhou, X. Ren, and Y. Hui. Effect of start position on human performance in steering tasks. In *2008 International Conference on Computer Science and Software Engineering*, vol. 2, pp. 1098–1101, 2008. doi: 10.1109/CSSE.2008.1310 3

[72] D. J. Zielinski, H. M. Rao, N. D. Potter, M. A. Sommer, L. G. Appelbaum, and R. Kopper. Evaluating the effects of image persistence on dynamic target acquisition in low frame rate virtual environments. In *2016 IEEE Symposium on 3D User Interfaces (3DUI)*, pp. 133–140, 2016. doi: 10.1109/3DUI.2016.7460043 1

[73] D. J. Zielinski, H. M. Rao, M. A. Sommer, and R. Kopper. Exploring the effects of image persistence in low frame rate virtual environments. In *2015 IEEE Virtual Reality (VR)*, pp. 19–26, 2015. doi: 10.1109/VR.2015.7223319 3

A Coefficients of Models Evaluation

Table 3: Detailed values of coefficients derived from nonlinear regression for each model with 95% CIs [lower, upper].

	a	*b*	*c*	*d*	*e*	*f*
BL1	906.93 [636.23. 1177.87]	113.50 [79.43, 147.57]				
BL2	1098.61 [991.988, 1205.35]	646.76 [562.52, 730.99]				
BL3	1073.21 [865.97, 1280.35]	57.81 [32.34, 83.29]	-2572.24 [-3071.85, -2072.29]			
BL4	576.73 [354.45, 739.02]	100.71 [77.84, 123.57]	1198.77 [793.13, 1604.45]	-82.12 [-87.98, -76.32]		
CM1	4.57 [-157.46, 166.60]	331.45 [241.83, 421.07]	-945.30 [-1871.61, -18.99]	-68.16 [-75.25, -61.07]	10.55 [3.10, 18.00]	0.34 [0.26, 0.42]
CM2	485.72 [396.85, 574.52]	173.33 [109.31, 237.32]	1821.21 [1156.33, 2486.09]	-121.75 [-162.74, -80.75]	0.06 [-0.09, 0.23]	0.47 [0.13, 0.8]